X-525-67-495
PREPRINT

SIMULATION STUDY OF A PRECISE HYBRID SERVO CONTROL SYSTEM

GEORGE C. WINSTON
WILLIAM H. LONG

SEPTEMBER 1967

GODDARD SPACE FLIGHT CENTER
GREENBELT, MARYLAND

X-525-67-495

SIMULATION STUDY OF A PRECISE HYBRID SERVO CONTROL SYSTEM

George C. Winston

and

William H. Long

September 1967

GODDARD SPACE FLIGHT CENTER
Greenbelt, Maryland

SIMULATION STUDY OF A PRECISE HYBRID SERVO CONTROL SYSTEM

George C. Winston
and
William H. Long

SUMMARY

This report describes an analog computer simulation study of a precise hybrid (digital-analog) servo control system designed to control an experimental optical tracking mount. The control concept developed for this system was relatively unique at the time of its inception (March 1963) and no references to performance of similar systems were known. As a consequence a detailed simulation study was performed. This study indicated the soundness of the concept (since confirmed experimentally) and demonstrated a tracking capability well within the two arc second specification. Techniques were developed and demonstrated in the simulated system for overcoming nonlinear effects of amplifier saturation and coloumb friction.

TABLE OF CONTENTS

LIST OF FIGURES

TABLE OF SYMBOLS

C = Mount axis angle

$C(nT)$ = Mount axis angle at sample instant n

ΔC = Increment of C

D = Axis Damping

e = Servo error

F = Bi-directional counter content

$G_c(s)$ = Compensation circuitry transfer function

$G_d(s)$ = Digital circuitry transfer function

G_m = Gain margin

$G_t(s)$ = Tachometer loop closed-loop transfer function

K = Loop Gain

K_A = Power Amplifier Gain

K_C = Compensation Network Gain

K_D = Digital Circuit Gain

K_M = Torque Motor Constant

K_P = Pre-amplifier Gain

K_T = Tachometer Sensitivity

N = Nonlinear function; also designates N^{th} sampling interval

R = Servo input command

$R(nT)$ = Servo input command at sample instant n

s = Laplace operator

T = Sampling period

ϵ = Mount motion required during the next sample period

ϵ' = Pulse frequency corresponding to ϵ

τ_1 = Compensation Time Constant

τ_2 = Compensation Time Constant

τ_e = Motor Electrical Time Constant

τ_m = Mount Mechanical Time Constant

ϕ_m = Phase Margin

SIMULATION STUDY OF A PRECISE HYBRID SERVO CONTROL SYSTEM

INTRODUCTION

This report describes an analog computer simulation study of a precise hybrid (digital-analog) servo control system designed to position an experimental optical tracking mount. The study was undertaken to determine the feasibility of a particular system concept and feasibility having been established to determine optimum parameter values.

The tracking mount employs an x-y axis configuration and supports a telescope tube having approximate dimensions of 14 feet in length and 3 feet in diameter and weighing approximately 3500 pounds. The telescope is flexible in design permitting the use of a variety of optical systems. The mount is to be used in support of various optical experiments, many employing laser optics having very narrow beamwidths. As a result performance requirements for the control system are severe. Briefly stated these are to provide dynamic pointing accuracies to within the apparent line-of-sight jitter produced by the atmosphere; i.e., to within one to two arc seconds, at axis velocities ranging from less than sidereal rate (15 arc seconds per sidereal second) to 3 degrees per second, and at accelerations ranging from zero to 0.15 degrees per second squared. Maximum velocity should be 5 degrees per second and maximum acceleration 2 degrees per second squared. An additional specification is for long term stability to permit extended time-exposure photography. The requirement is for an accumulated drift from a tracked object (a star or deep space probe moving at essentially sidereal rate) of less than 5 arc seconds over a tracking period of one hour. This specification requires the establishment and maintenance of an axis rate to within one part in 10^{-4}.

SYSTEM DESCRIPTION

The resolution, repeatability and low drift rates required led to a consideration of digital techniques for this application. As a consequence a system concept based upon frequency modulation of a pulse train as the information media was developed. The pulse frequency modulation (PFM) technique has the advantage of permitting control information to be processed by relatively simple, discrete digital circuitry. In this system the digital circuits perform a portion of the system compensation including one integration. The presence of this integration in the driftless digital circuits eliminates all significant effects of long

term drifts in the following analog compensation circuitry. A further advantage of the PFM technique is that since a pulse is generated for every detectable (quantum) change in the data value the system is equivalent to a sampled data system having an infinite sampling rate. The infinite equivalent sampling rate eliminates problems inherent to conventional sampled data systems wherein a finite sampling rate introduces phase lag and frequency folding, resulting in degradations in system stability and accuracy.

The control system provides a high degree of flexibility in using the mount by means of several operating modes. These modes include programmed drive from data stored on a punched paper tape, fixed rate sidereal drive, manual control of position and velocity and combinations of all of these. Details of the system configuration are unique to each mode, of course, but all are based upon the block diagram of Figure 1. This is the configuration of the program mode and encompasses all of the accuracy and stability problems which require simulation study. The other modes differ primarily in the manner in which command data is derived.

Referring to Figure 1, it is seen that there are three loops, the inner one being an analog velocity loop closed by means of a high quality dc tachometer. The primary purposes of this loop are to linearize the motor and bearing characteristics and to reduce the apparent mechanical time constant.

The control system employs an encoder which has both an absolute angle output, $C(NT)$, and an incremental output, ΔC, in the form of a pulse for each quantum (0.001°) of shaft rotation. Physically these pulses appear on one of two lines depending upon the direction of rotation. The second loop is closed by the encoder's pulse output. This is an incremental position loop which moves the mount one encoder quantum of rotation for each pulse of the command pulse train ϵ'. The command pulses are also distinguished as to direction of rotation and are counted by the bi-directional counter. The instantaneous number in the counter is converted to an analog voltage which drives the mount after compensation. Rotation of the mount axis results in encoder incremental pulses which are applied to the counter in the sense to oppose the command pulses. When the mount has moved through the required angle the counter content is zero. By applying a continuous command pulse train to the incremental loop the mount may be made to turn at a constant desired rate.

The outer loop is closed by the absolute angle encoder output $C(NT)$. This angle feedback is sampled once per second. The input to the loop consists of discrete time command angles which may, for example, be predictions of a spacecraft's position at specific times. These angles are also read at a rate of once per second, but in this case one sample period ahead of real time, and are designated $R[(N+1)T]$.

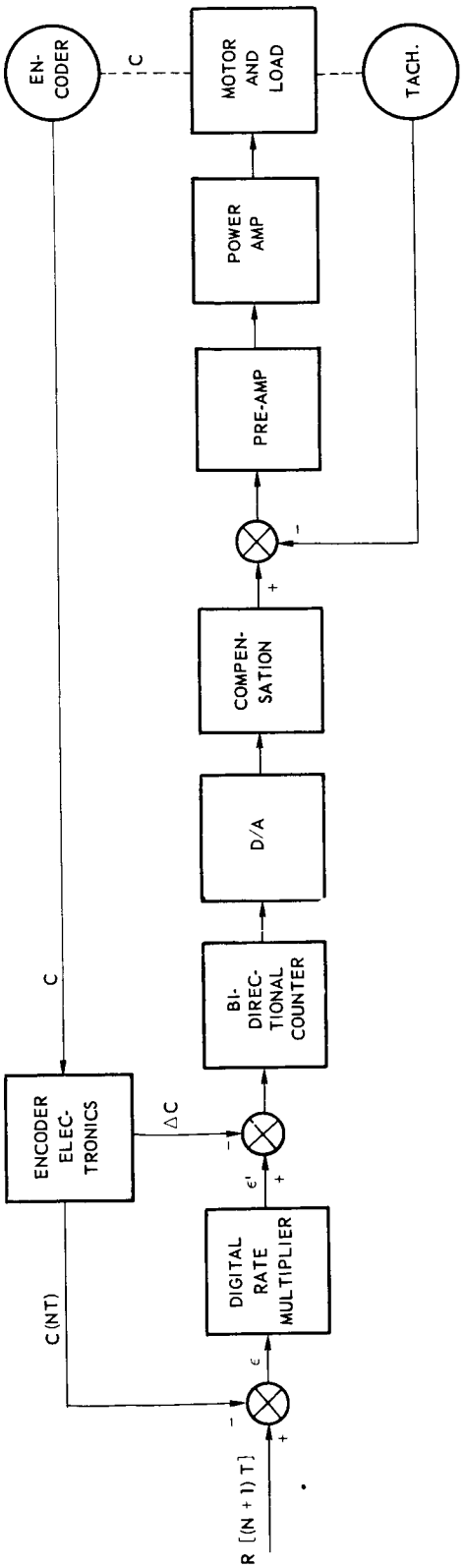

Figure 1. Block Diagram of Control System (One Axis)

The difference between C(NT) and R[(N + 1) T], designated ϵ, is the motion desired during the next second and is the sum of the predicted change of the line-of-sight angle and the present servo error. This difference angle is applied to a digital rate multiplier [1] which produces a pulse train with pulse repetition rate proportional to the input number. The incremental loop is thus driven at a rate which causes the mount's axis angle to arrive at R[(N + 1) T] at the end of the sample period.

It should be noted that the digital subsystem performs a linear interpolation of the input sampled data. This permits a relatively low sample rate. The interpolation is made with the maximum resolution consistent with the encoder. A more accurate fit to the spacecraft trajectory is possible with a modified rate multiplier which makes a curvilinear fit to the sampled data input.[2]

SYSTEM ANALYSIS

To facilitate the derivation of the control system transfer function the system is divided into three categories: the digital circuits, the analog compensation and the tachometer loop. These are discussed below. The transfer function of the digital circuits is derived as follows*: The input to the rate multiplier, ϵ, is a number equal to the difference (in quanta) between the present axis angle C(NT) and the angle R[(N + 1)T] which is desired T seconds hence.

$$\epsilon(NT) = R[(N+1)T] - C(NT) = [R(NT) - C(NT)] + \{R[(N+1)T] - R(NT)\} \quad (1)$$

The rate multiplier produces a pulse train whose pulse frequency $\epsilon'(NT)$ is

$$\epsilon'(NT) = \frac{1}{T}\epsilon(NT) \quad (2)$$

When this pulse train is accumulated in the bi-directional counter the counter content due to ϵ is

$$F_\epsilon(t) = \sum_{n=0}^{N-1} e(nT) + \frac{\tau}{T} e(NT) + \frac{1}{T} \sum_{n=0}^{N-1} \{R[(n+1)T] - R(nT)\} + \frac{\tau}{T}[R(N+1)T - R(NT)] \quad (3)$$

*This derivation is due to R. V. Monopoli, University of Massachusetts, Amherst, Mass.

where $e(nT) = R(nT) - C(nT)$ and $\tau = t - NT$. The first two terms on the right hand side of (3) are the accumulated error to the beginning of the N^{th} sample period and the accumulated error within the N^{th} period, respectively. The sum of the last two terms of (3) are similarly the value of $R(t)$. In a like manner the encoder feedback pulses are accumulated in the counter to produce a negative term $C(t)$. Thus the total counter content is

$$F(t) = \sum_{n=0}^{N-1} e(nT) + \frac{\tau}{T} e(NT) + e(t); \quad N \geq 1 \tag{4}$$

A block diagram representation of (4) is given in Figure 2. The transfer function for the sample and hold is

$$\frac{1 - e^{-Ts}}{s} \tag{5}$$

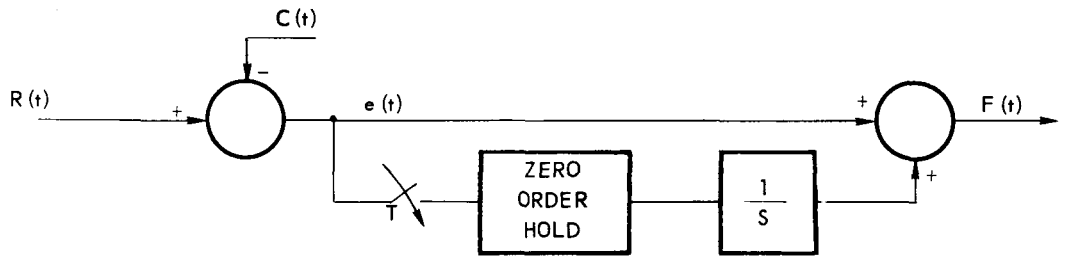

Figure 2. Diagram for Digital Transfer Function Derivation

The exponential may be expressed in series form so that (5) becomes

$$\frac{Ts - \frac{(Ts)^2}{2!} + \frac{(Ts)^3}{3!} - \cdots}{s} \tag{6}$$

The first two terms of (6) are used as an approximation (valid at low frequencies) to the transfer function of the sample-hold combination. Thus an approximate transfer function $F(s)/E(s)$ is

$$\frac{F(s)}{E(s)} \approx 1 + \frac{Ts - \frac{(Ts)^2}{2!}}{s^2} = \frac{(2 - T^2)\left(s + \frac{2T}{2 - T^2}\right)}{2s} \tag{7}$$

Setting $T = 1$ second and multiplying by K_D gives the digital circuit transfer function,

$$G_d(s) = K_D\left(\frac{0.5s + 1}{s}\right) \tag{8}$$

The transfer function of the analog compensating circuit is as follows:

$$G_c(s) = \frac{K_C(\tau_1 s + 1)^2}{s(\tau_2 s + 1)} = \frac{8(0.8s + 1)^2}{s(3s + 1)} \tag{9}$$

Observe that part of the compensation (Equation 8) is performed in the digital circuits where gain as well as a pure integration and a zero are added to the system transfer function.

The compensating circuit was first designed using Bode and root locus procedures and then verified on the computer. From the Bode plot, shown in Figure 3, it can be seen that with this particular choice of compensation the phase margin is 64 degrees and the gain margin is 18 decibels and the bandwidth is 17 radians per second.

A simplified block diagram of the X-axis system (Figure 4) may now be drawn where:

K_D = Digital Circuit Gain = 12 volts/degree.

K_C = Compensation Network Gain = 8 volts/volt.

K_P = Pre-amplifier Gain = 10 volts/volt.

K_A = Power Amplifier Gain = 200 volts/volt.

K_M = Torque Motor Sensitivity = 6.25 lb-ft/deg/sec.

K_T = Tachometer Sensitivity = .715 volts/deg/sec.

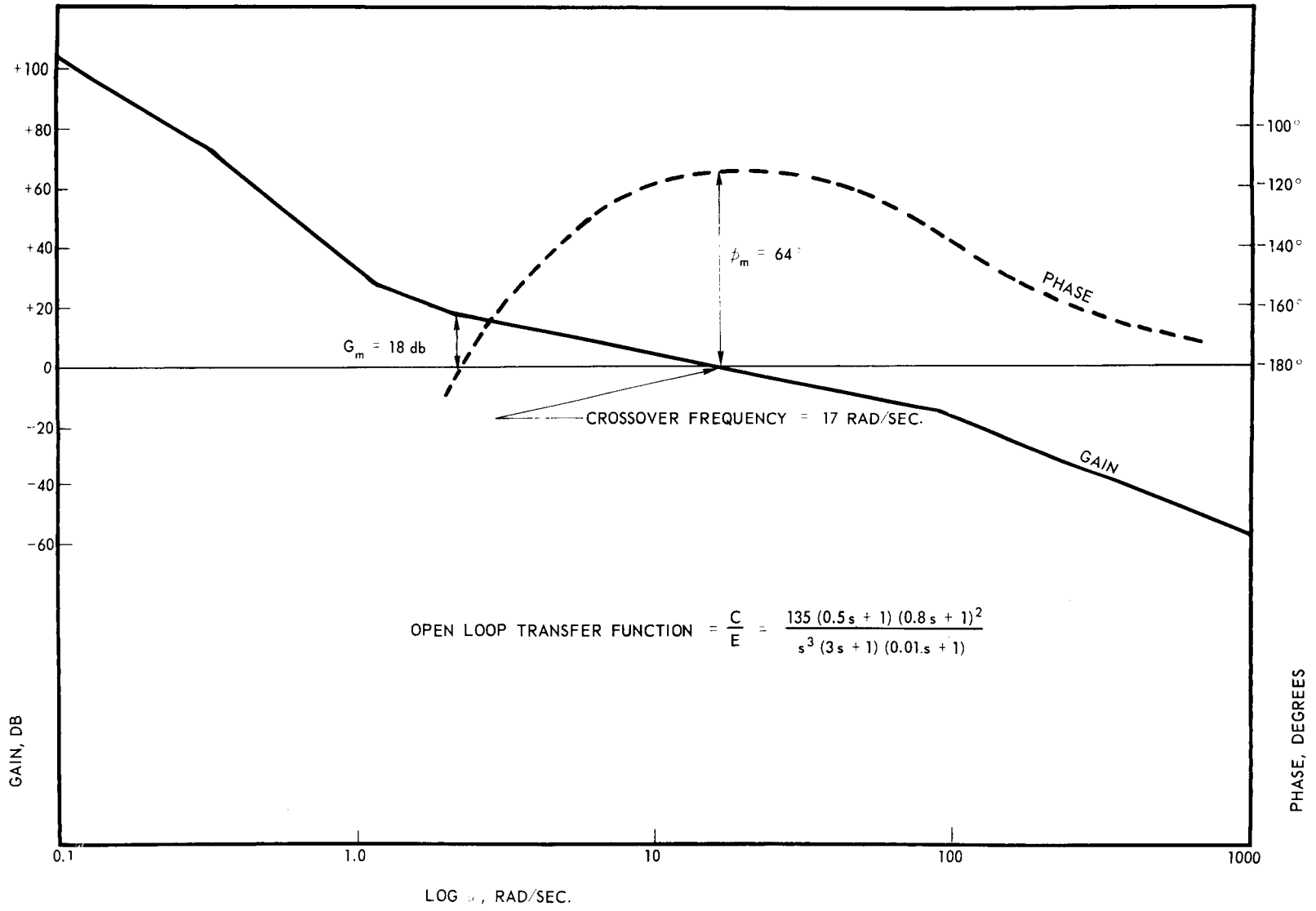

Figure 3. Bode Plot

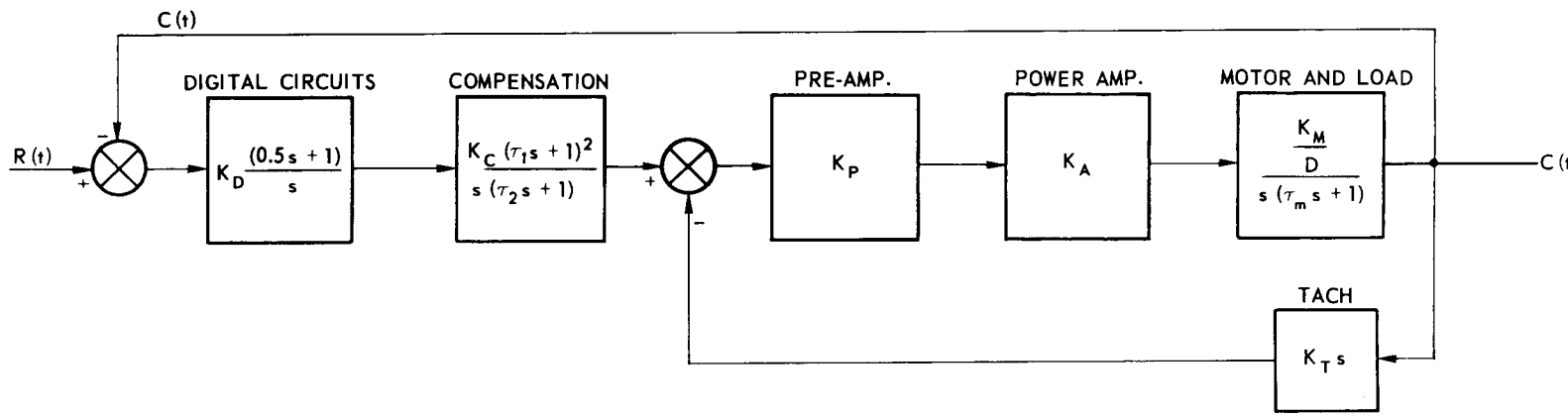

Figure 4. Simplified Block Diagram

D = Axis Damping = 8.95 lb-ft/deg/sec.

τ_e = Motor Electrical Time Constant = 0.035 sec.

τ_m = Mount Mechanical Time Constant = 11.8 sec.

τ_1 = Compensation Time Constant = 0.8 sec.

τ_2 = Compensation Time Constant = 3 sec.

It should be noted that $\tau_e << \tau_m$ and can be neglected.

Since the preamplifier, power amplifier and motor are enclosed by a feedback loop, the closed loop transfer function of this loop must be determined in order that the open loop transfer function of the system can be found. The closed loop transfer function of the tachometer loop is:

$$G_t(s) = \frac{\dfrac{K_P K_A K_M}{Ds(\tau_m s + 1)}}{1 + \dfrac{K_P K_A K_M K_T}{D(\tau_m s + 1)}} = \frac{1.4}{s(0.01s + 1)} \qquad (10)$$

For the case of a sampling rate of one per second, the open loop transfer function of the system becomes:

$$G_s(s) = K_D\left(\frac{0.5s+1}{s}\right) \times \frac{8(0.8s+1)^2}{s(3s+1)} \times \frac{1.4}{s(0.01s+1)} = \frac{135(0.5s+1)(0.8s+1)^2}{s^3(3s+1)(0.01s+1)} \qquad (11)$$

Since the position loop has three integrations, the servo is classified as a type 3 system; therefore, the steady state errors due to position, velocity and acceleration are all theoretically zero.

ANALOG COMPUTER SIMULATION

The transfer function of the system was simulated on the computer as shown in Figure 5. The sample and hold function of the digital circuit was simulated by a motor driven switch and a hold circuit. The circuit samples the signal at point A at one second intervals and holds it for one second. Because of the wide

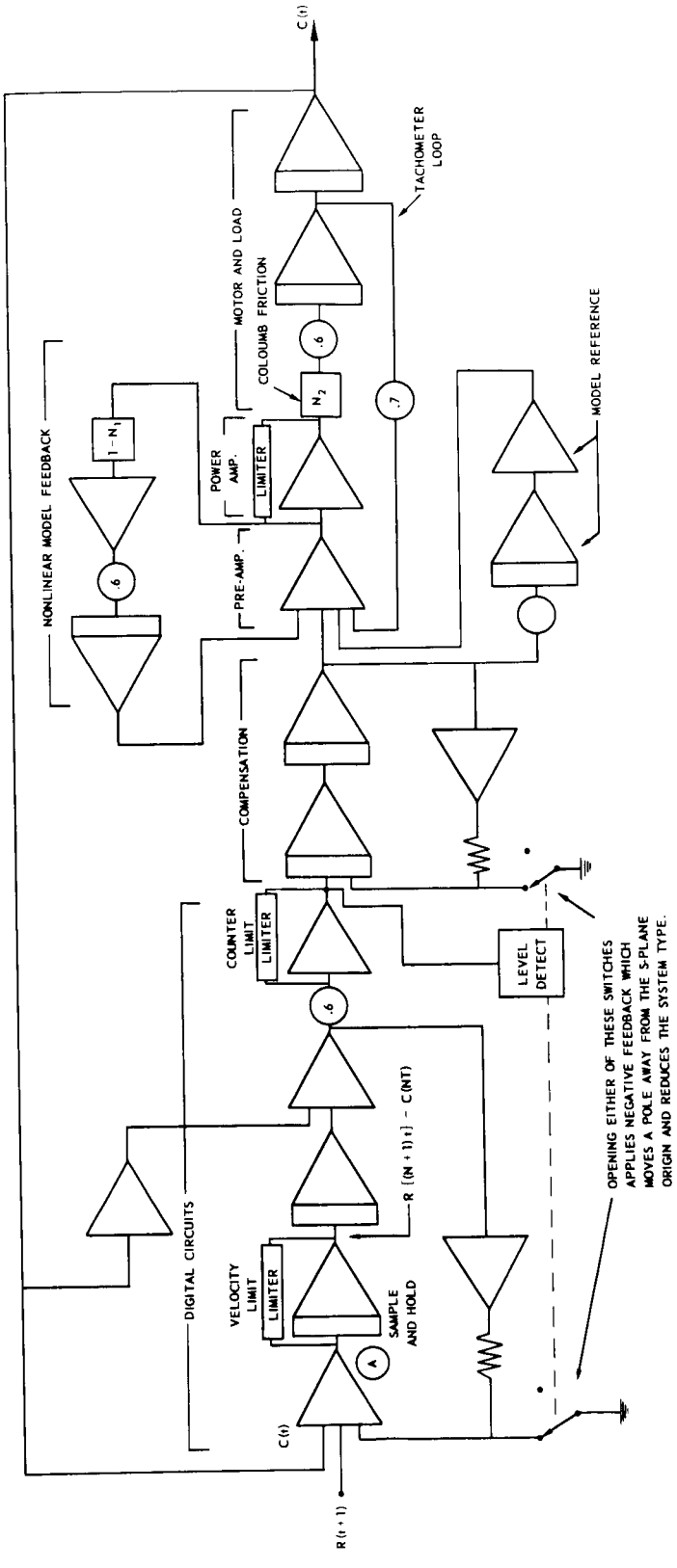

Figure 5. Analog Computer Simulation

dynamic range of the system it was necessary to use different analog computer scalings for large signal and small signal studies. Digital quantization was not simulated due to its small magnitude.

It was anticipated that the real system would have four principle nonlinearities. They are as follows:

1. Coloumb friction due to the torque motor brushes and the bearings. This condition was simulated by a dead-zone element (N_2 in Figure 5) in series with the motor input. The stiction is very nearly equal to the coloumb friction, according to manufacturer's data; therefore, it was neglected in the simulation.

2. Power amplifier saturation (N_1 in Figure 5). This was simulated by a shunt limiter across the computer amplifier which represents the power amplifier in the real system.

3. Saturation of counter output. Since the maximum voltage out of the digital-to-analog converter is ± 3 volts, the counter is limited to ± 500 counts in order that the volts per count will be as high as possible. The amplifier output representing the output of the digital circuits reflects this limit.

4. Rate multiplier limit. The rate multiplier is purposely bounded in order to provide a velocity limit of five degrees per second. A limit is included in the digital approximation which represents the velocity limit.

Because of the very high accuracy requirements placed on the system, the effects of the nonlinearities become major problems, whereas in normal systems they are less serious. Two major problems arose when these nonlinearities were included in the simulation: (1) large signal instability, and (2) a limit cycle. These will be discussed separately below:

Since the system is a type 3 servo it is sensitive to large signal shocks such as step inputs and switching transients. It was anticipated that these transients would occur only during slewing and start-up and would present no problems during normal tracking. It thus was necessary to devise a means of reducing the order of the servo system during transient periods. This was done by applying negative feedback around the integrations in the digital circuits and compensating network (see Figure 5). The closed loop transfer function of these loops becomes approximately unity and the system is a type 1 servo with a low loop gain. The system switches to a type 1 system when the output of the digital

circuits nears saturation, indicating a large error. When the output returns to some nominal low value the system switches to a type 3 system.

The transient introduced when the system switches from a type 1 to a type 3 was large enough to cause the system to go into oscillations because of power amplifier saturation. A scheme was tried which allowed the system to switch from a type 1 to a type 2 to a type 3 in a timed sequence, but again, the transients caused instability.

One successful solution to the problem was found by applying nonlinear model feedback around the power amplifier. Figure 6 shows the block diagram

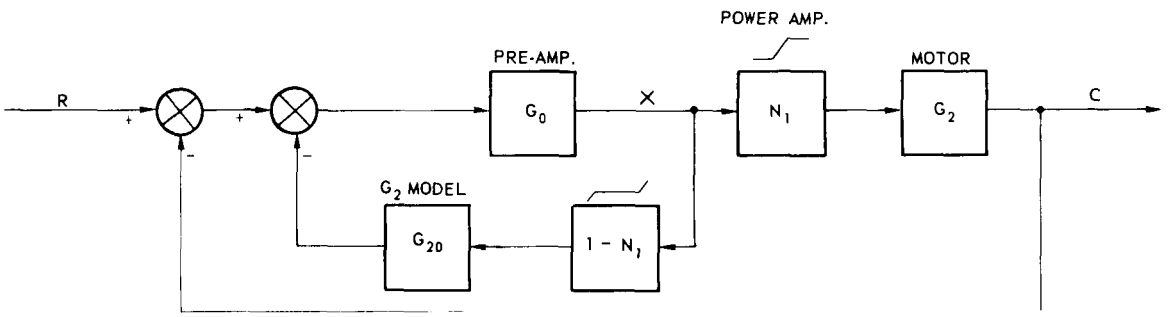

Figure 6. Nonlinear Model Feedback

for this scheme.[3] Power amplifier saturation is designated by N_1. The intentionally introduced nonlinearity $(1 - N_1)$ is developed by a diode function generator and is the complement of N_1. A small signal X sees N_1 as a linear function and $(1 - N_1)$ as an open circuit. As X increases in amplitude saturation is reached in N_1. At the same time, however, $(1 - N_1)$ begins to pass a signal which is just that part of X which N_1 has clipped. To the extent that G_2-model duplicates G_2 the total feedback is continuous and linear. The mount still exhibits the effects of torque saturation but large signal instability is avoided. The nonlinear feedback in the simulation is shown in Figure 5. The results from the simulation indicate that the effectiveness of the nonlinear feedback is relatively independent of how well G_2-model equals G_2. Varying the time constant and gain of G_2-model by ± 5 times that of G_2 had little effect on system performance.

The second nonlinearity considered in the simulation is that of the coulomb friction. This condition causes the system to oscillate in a limit cycle when the

mount is standing still or moving at a slow rate. Three approaches to this problem were tried. First, the gain of the tachometer loop was raised to a high value (50K) which resulted in a reduction of the limit cycle magnitude, but the high gain caused serious noise problems. Second, dither was summed into the tachometer loop. The dither also reduced the limit cycle; but because of uncertainties as to the effect of dither on the optical equipment, it was abandoned. Third, a model reference was used in the tachometer loop as shown in Figure 7.

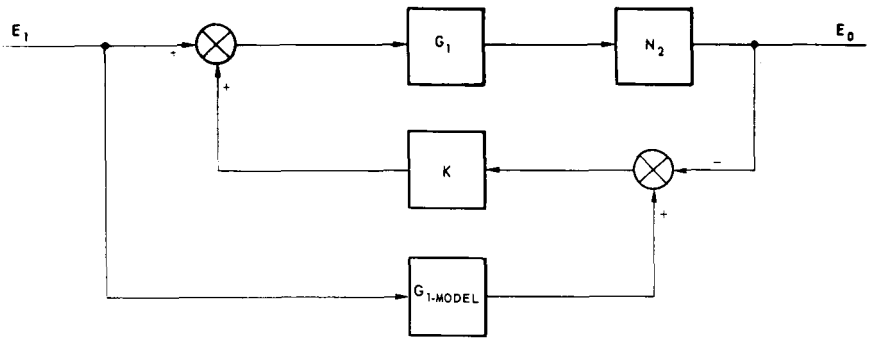

Figure 7. Model Reference

G_1 is the linear closed loop transfer function of the tachometer loop and N_2 is the describing function of the coulomb friction. This circuit compares the output of the nonlinear system to that of an idealized, linear model. The difference is amplified and applied to the input of the nonlinear system with a polarity to force the system output toward agreement with the model output. This is confirmed by the transfer function derived from Figure 7 as follows:

$$E_0 = \left[G_1N_2 + (G_{1\text{-MODEL}})\, KG_1N_2\right] E_1 - KG_1N_2E_0 \tag{12}$$

$$\frac{E_0}{E_1} = \frac{G_1N_2\left[1 + K(G_{1\text{-MODEL}})\right]}{1 + KG_1N_2} \tag{13}$$

If $G_{1\text{-MODEL}} \simeq G_1$ and $K >> 1$

$$\frac{E_0}{E_1} \simeq G_1 \tag{14}$$

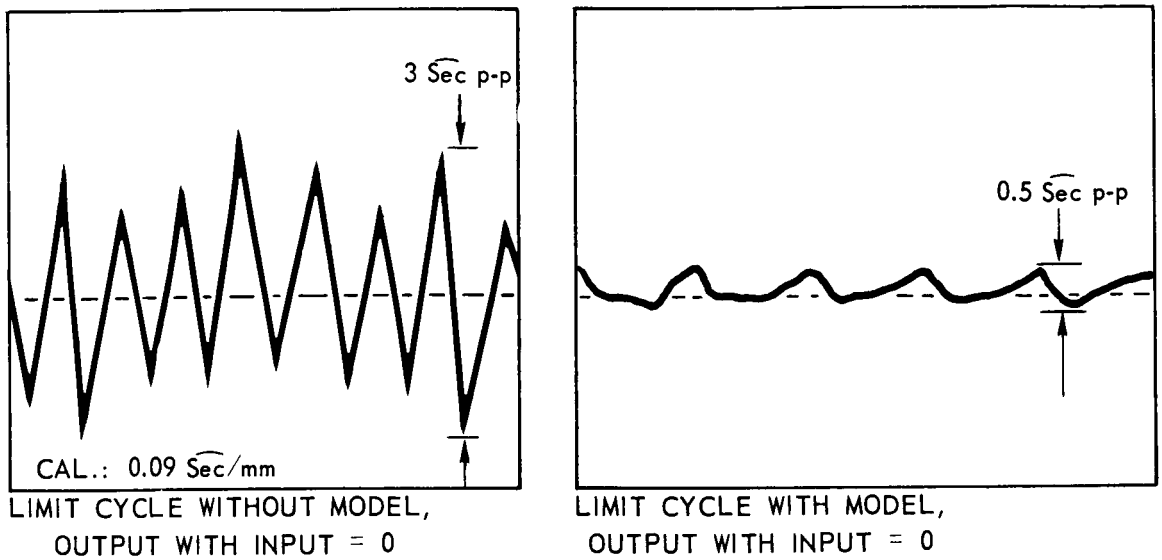

Figure 8. Effect of Model Reference on Limit Cycle

From the response curves shown in Figure 8 it can be seen that this scheme reduced the limit cycle from about ±1.5 arc seconds to ±0.25 arc seconds. In addition to reducing the limit cycle the model reference reduces the effect of noise in the tachometer loop considerably as can be seen from the plots in Figure 9.

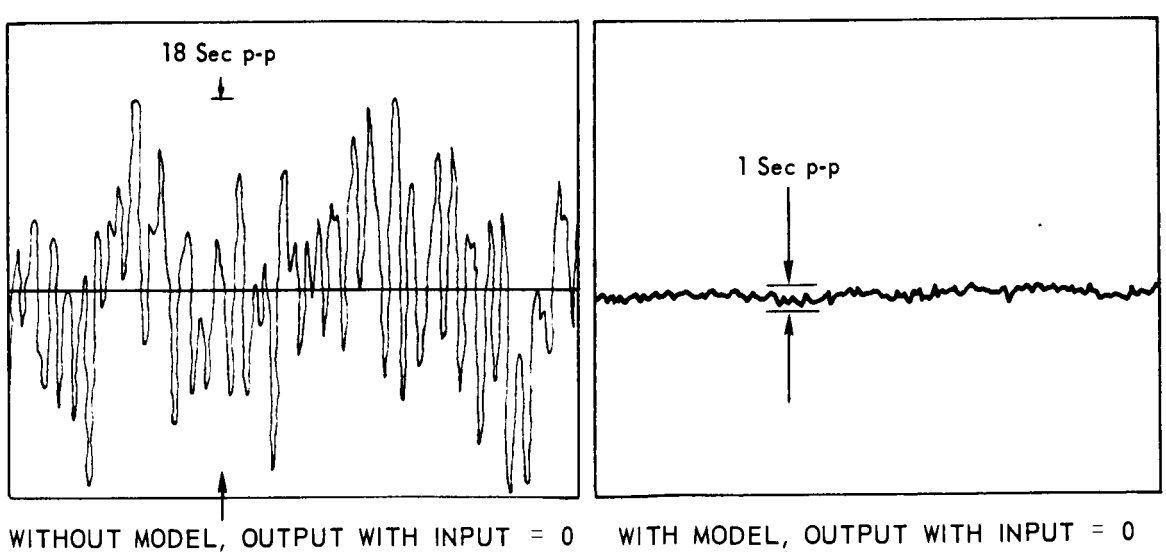

Figure 9. Effect of Model Reference on Noise Summed into Tachometer Loop

Again, the simulation indicated that the effectiveness of the model is relatively independent of how well the model of G_1 equals the true G_1 over a range of agreement that should be readily achieved in practice.

COMPUTER SIMULATION RESULTS

With the computer implemented as shown in Figure 5, various tests were conducted to determine if the control system could meet the specifications. Some of these tests are described below.

The system response to a step of position and velocity is shown in Figure 10. Note that the output response lags the position command by one second, verifying that the position command is truly $R[(N+1)t]$.

From Figure 5 it can be seen that there is no point at which the error $[R(t) - C(t)]$ can be measured directly. In order to measure the error for various loop gains, it was necessary to change the digital approximation by simulating the transfer function without the sampling. The position command then becomes $R(t)$ (the position command at time t) and the error can be measured directly. The results are shown in Figure 11. When the loop gain is 135 the error is small (1.5 arc seconds maximum), but when it is decreased by a factor of four the error becomes appreciable (5.4 arc seconds). The input is a 0.01 cps sine wave which has position and velocity components comparable to those of a satellite in a 100-mile circular orbit. The simulated acceleration component, however, is about three times too great theoretically and even more for the distorted sine wave input shown. Hence, the simulated input is worse than that encountered in normal tracking, giving a conservative result.

Several other tests with the simulation were conducted as follows:

1. Various system parameters (τ_m, K_T, N, D) were varied over fairly large ranges to determine the effect of such changes on system performance. The results indicate the performance is not degraded appreciably by parameter variation, hence, the simulation should be fairly good over a wide range of real system parameters.

2. A closed loop frequency response test was conducted which indicated a bandwidth of 2.5 cycles per second.

3. A Gaussian noise generator was used to simulate noisy conditions in the digital circuits by summing noise into the digital circuits output. The results indicate that noise of Gaussian type will have a noticeable effect

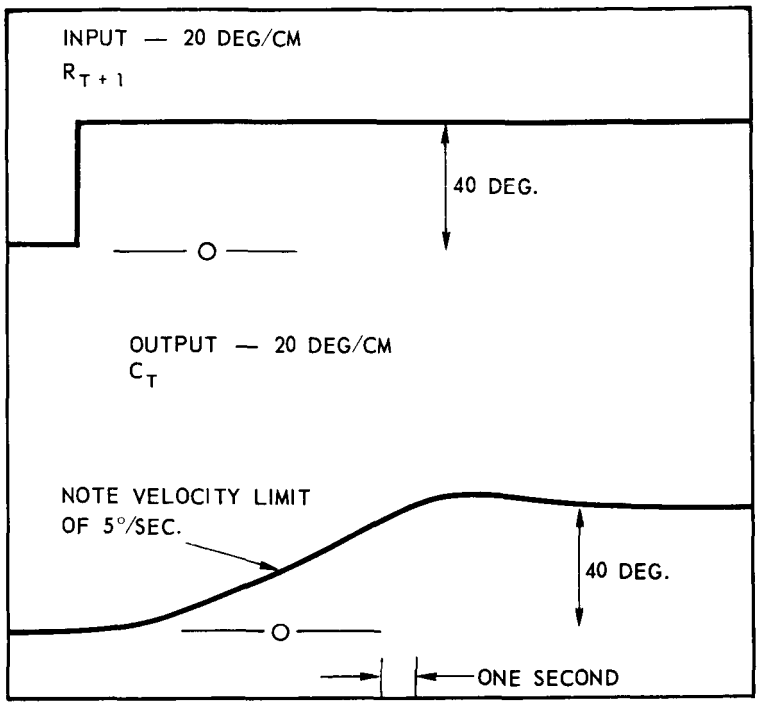

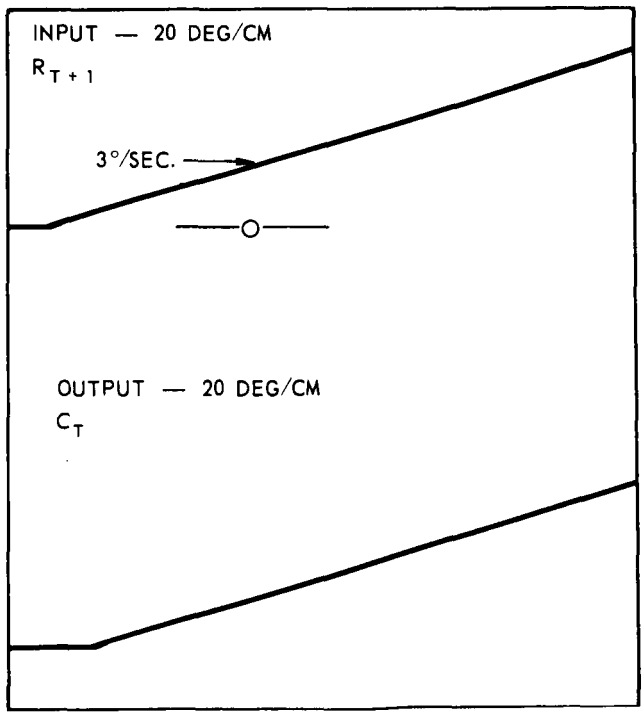

Figure 10. System Transient Response

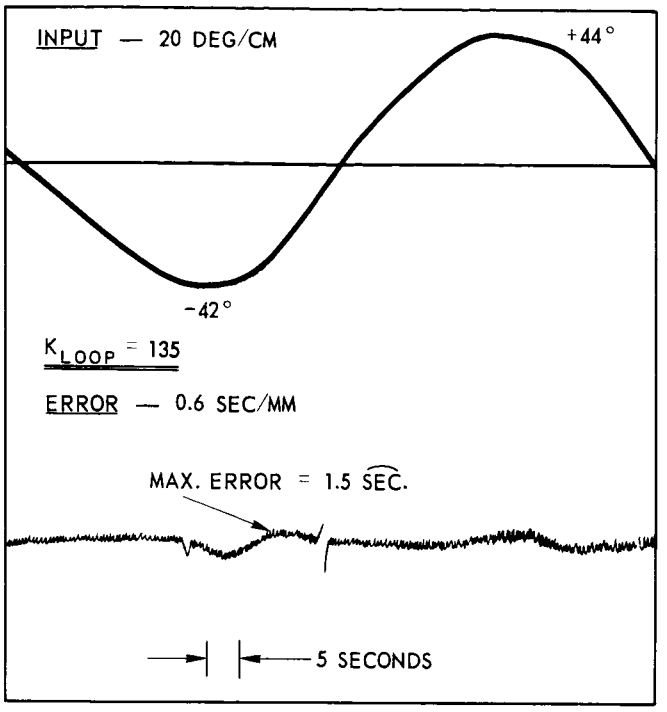

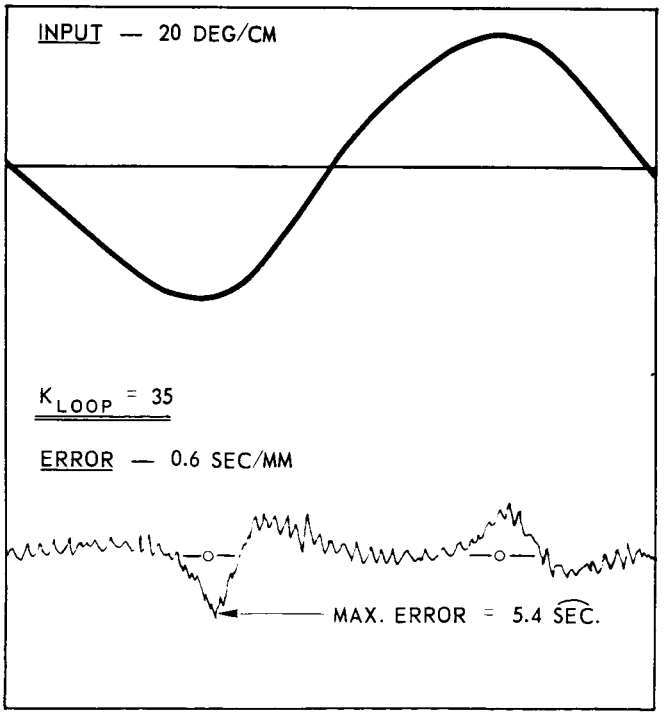

Figure 11. System Tracking Error

on the system output and that pains must be taken to develop a clean signal at this point.

4. Low frequency sine waves (.001 cycles per second) were summed into the tachometer loop to simulate amplifier drift. The frequency of these drifts is well within the servo bandwidth, therefore, the servo compensates for them.

CONCLUSION

Results of the simulation study indicated that the system as designed would meet the specifications. Modeling techniques were developed which demonstrated the ability to cope with nonlinearities considerably more severe than expected in practice. Whether these techniques will have to be incorporated in the final system will be determined by experimental results.

Since completion of this study the system has been built. It is undergoing thorough testing at this time. Results from these tests will be published in the near future.

REFERENCES

1. Digital Linear Interpolation and the Binary Rate Multiplier, W. Arnstein, H. W. Mergler and B. Singer, "Control Engineering", June 1964.

2. A Digital Rate Multiplier for Curvilinear Interpolation of Sampled Data, G. C. Winston, NASA Report No. X-525-67-277, June, 1967.

3. Adaptive Control Systems, E. Mishkin and L. Brann, Jr., McGraw-Hill Book Company, New York, 1961, pp. 204-207.